

Evidence That tRNA Synthetase-Directed Proton Transfer Stops Mistranslation

William F. Waas and Paul Schimmel*

Department of Molecular Biology and The Skaggs Institute for Chemical Biology, The Scripps Research Institute,
10550 North Torrey Pines Road, La Jolla, California 92037

Received April 22, 2007; Revised Manuscript Received August 21, 2007

ABSTRACT: To prevent mistranslation, aminoacyl-tRNA synthetases (AARSs) discriminate against noncognate amino acids and cellular metabolites. Defects in specificity produce statistical proteins which, in mammalian cells, lead to activation of the unfolded protein response and cell death. Because of inherent limitations in amino acid discrimination by a single active site, AARSs evolved a separate domain to clear mischarged amino acids. Although the structure of a widely distributed editing domain for ThrRS and AlaRS is known, the mechanism of amino acid clearance remains elusive. This domain has two motifs that together have four conserved residues in the pocket used to clear serine from mischarged tRNAs. Here, using ThrRS as an example, rapid single-turnover kinetics, mutagenesis, and solvent isotope analysis show that a strictly conserved histidine (between ThrRS and AlaRS) extracts a proton in the chemical step of the editing reaction. Three other conserved residues, and two additional residues in the editing pocket, are not directly implicated in the chemical step. These results are relevant to the previously reported mutagenesis of the homologous editing pocket of alanyl-tRNA synthetase, where even a mild defect in editing causes neurodegeneration in the mouse. Thus, a single proton-transfer event needed to prevent mistranslation can have profound implications for disease.

The genetic code is an ancient and universal algorithm for expression of proteins from nucleic acid sequences. The rules of the genetic code are governed by biochemical reactions that link the 64 codon triplets to a set of 20 amino acids and 4 polypeptide start/stop signals. A set of ligated adaptor molecules, aminoacyl-tRNAs, physically link individual amino acids to their respective anticodon sequences. These linkages are established by aminoacyl-tRNA synthetases (AARS)¹ that relate the structural and chemical nature of an amino acid to the unique identity elements of its cognate tRNA. In this way, the rules of the genetic code are established. At the same time, when the rules are broken, mistranslation occurs and that, in turn, can lead to disease.

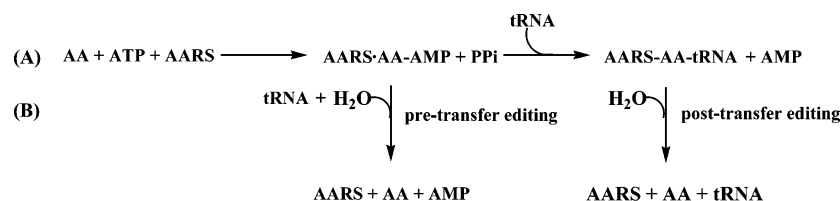
Errors in AARS-mediated amino acid selection produce mismatched amino acid-anticodon pairs in the form of misacylated tRNA. These mischarged tRNAs cause mistranslation that leads to production of statistical polypeptides. Mistranslation has significant consequences in vivo. For example, enhanced misincorporation decreases cell viability and can lead to cell death in prokaryotes (1, 2). And in mammalian cell culture, an apoptotic-like response is induced (3). In another example, the *sti* mutation, which marginally compromises alanyl-tRNA synthetase (AlaRS) specificity, triggers the unfolded protein response and leads to neurodegeneration in the mouse (4).

Aminoacylation of tRNA is a two-step process. Using a single active site, AARSs activate amino acids and transfer them to ribose (2'- or 3'-hydroxyl) of a tRNA terminal adenosine (A₇₆) (Scheme 1A). Thermodynamic arguments contend that this mechanism has specificity limitations (5). These limits are readily apparent for several AARSs (AlaRS, IleRS, LeuRS, ThrRS, and ValRS), each of which must select among structurally similar amino acids. For example, at equal concentrations in vitro, isoleucyl-tRNA synthetase (IleRS) misactivates approximately 1 valine for every 200 isoleucines. However, misincorporation in vivo occurs at a rate of less than 1 in 3000 (6). The difference is explained by hydrolytic editing activities which correct misactivation and misacylation events.

The 20 AARSs are divided into two classes of 10 enzymes each. These classes are defined by the class-specific architecture of the respective active site. Hydrolytic proofreading mechanisms are known for both class I and class II AARSs (7–11). In these instances, two distinct modes of proofreading (or editing) have been described: hydrolysis of misactivated aminoacyl adenylates (pretransfer editing) and/or misacylated tRNAs (post-transfer editing) (Scheme 1B) (12, 13). Pretransfer editing is exclusive to a subset of AARSs, whereas post-transfer editing occurs more generally (7–9). These activities are localized to active sites that are distinct from and distal to (~30 Å) those used for aminoacylation (10). To date, six structurally distinct editing domains have been identified: a domain (ED_{CI}) associated with class I enzymes like IleRS, ValRS, and LeuRS, a domain (ED_{CIa}) found in class II enzymes like AlaRS and ThrRS, an archaeal-specific module (ED_{CIb}) associated with class II synthetases, and structures associated with ProRS and PheRS (14–25).

* To whom correspondence should be addressed. Phone: (858) 784-8972. Fax: (858) 784-8990. E-mail: schimmel@scripps.edu.

¹ Abbreviations: AARS, aminoacyl-tRNA synthetase; ThrRS, threonyl-tRNA synthetase; AlaRS, alanyl-tRNA synthetase; IleRS, isoleucyl-tRNA synthetase; ValRS, valyl-tRNA synthetase; LeuRS, leucyl-tRNA synthetase; AlaXp, Ala-X protein; SerAdn, seryl-3'-aminoadenosine; KSIE, kinetic solvent isotope effect; Ser-tRNA^{Thr}, serylated, threonine-specific tRNA.

Scheme 1: General Reaction Mechanism for Aminoacyl-tRNA Synthetases^a

^a AA, amino acid; tRNA, transfer ribonucleic acid; AA-AMP, aminoacyl-adenylate; AA-tRNA, aminoacyl-tRNA.

The ED_{CIIa} architecture not only appears as part of eukaryotic and bacterial AlaRS and ThrRS but also exists in proteins that closely resemble (in sequence) EDC_{IIa} of AlaRS but lack aminoacylation activity (AlaXps). All EDC_{IIa}'s have in common two signature sequence motifs (HXXXXH and CXXXXH). They also catalyze the same reaction, i.e., hydrolysis of serine from the 3'-end of their cognate tRNAs (ThrRS deacylates SertRNA^{Thr}, whereas both AlaRS and AlaXps hydrolyze Ser-tRNA^{Ala}) (14, 23, 26). ED_{CIIa} is hypothesized to have originally existed as a free-standing module that was later recruited to the early AlaRSs and ThrRSs (27).

The goal of this study was to provide insights into the kinetic mechanism of the ED_{CIIa} domain, in light of what is known about the protein structures. An understanding of this relationship may help to explain disease-causing mutations in proteins of the translation apparatus, as well as provide a basis for expansion and engineering of the genetic code. *E. coli* threonyl-tRNA synthetase (ThrRS_{EC}) was chosen for this study because many of its biophysical properties are well-characterized and several crystal structures are available, including a high-resolution structure of its ED_{CIIa} in the presence of seryl-3'-aminoadenosine (SerAdn), a post-transfer editing substrate analogue (14, 28–31). This structure provides a snapshot of the active editing conformation. Collectively, these studies provided a strong foundation for functional analysis of ED_{CIIa}-mediated editing.

A rapid-kinetic assay was used to directly monitor the hydrolysis of misacylated tRNA. The rapid-kinetic method was then applied to a mutational analysis of the catalytic mechanism of ED_{CIIa}. Stopping mistranslation was shown to be critically dependent on a single ionization constant and rate-limiting proton transfer. Because the site of ionization is strictly conserved in ThrRSs and AlaRSs, and because of the connection of an editing defect in mouse AlaRS to neuropathology, the results illustrate how disruption of a single ionization event for editing can have profound consequences for disease.

MATERIALS AND METHODS

Buffers, Reagents, and Strains. All buffers and chemicals were purchased from Sigma (St. Louis, MO) unless otherwise noted. Aminoacylation of tRNA^{Thr} was performed with [³H]-serine or [³H]threonine from ICN (Costa Mesa, CA). Ligase, Pfu Turbo polymerase, and restriction enzymes were obtained from Invitrogen Corporation (Carlsbad, CA). *Escherichia coli* DH5α (Invitrogen) was used for cloning, and *E. coli* BL21-DE3 (pLysS from Novagen (Madison, WI) was used for protein expression. Transfer RNA was expressed in *E. coli* MRE600 (ribonuclease I deficient strain). This strain was a gift from Barry S. Cooperman, University of Pennsylvania.

Preparation, Overexpression, and Purification of Native tRNA^{Thr}. The *thrW* gene was amplified by PCR from *E. coli* K12 genomic DNA under standard PCR conditions (1 min at 95 °C, 1 min at 53 °C, 1 min at 68 °C for 30 cycles), using the oligonucleotide primers P1 (5'-tataataaacGAATTCcgtgaacatgtccttcagg-3') and P2 (5'-aagaagaaaGGATC-Cttgtgtgggagaatgataagatc-3'). The amplified product was agarose-gel-purified and then digested and ligated into pEXT20, using BamHI and EcoRI restriction sites to create plasmid pWFW1015.

MRE600 cells were transformed with pWFW1015 by electroporation. A single colony was used to inoculate 25 mL of LB-ampicillin (100 μg/mL) and grown at 30 °C overnight. The culture was diluted (40-fold) into fresh LB-amp (1 L). Cells were grown at 30 °C to an OD₆₀₀ of 0.5 and induced with IPTG (1 mM, final). After 12 h of induction (30 °C), the cells were harvest by centrifugation.

Cell pellets were resuspended in 100 mL lysis buffer TL (0.3 M sodium acetate (pH 4.3), 10 mM EDTA) and mixed with an equal volume of water-saturated phenol. After shaking for 10 min, the phases were separated by centrifugation (10 000g, 30 min). Nucleic acids were then precipitated from the aqueous layer with ethanol. The precipitate was recovered by centrifugation (10 000g, 30 min), washed in neat ethanol, and dried. The dried pellet was dissolved in 10 mL of DP1 buffer (5 mM MES (pH 5.5), 1) and applied to a DNAPAC-100 column equilibrated in the same buffer. RNA was eluted using a linear gradient to 100% DP2 (5 mM MES (pH 5.5), and 1 M NH₄Cl) over 60 min (at 10 mL/min); the threonine acceptance activity of each fraction was determined. Fractions containing high-purity tRNA^{Thr} (in excess of 1300 pmol/A₂₆₀) were pooled and dialyzed against RP1 (10 mM sodium phosphate (pH 4.5), 1 M sodium formate and 8 mM MgCl₂). Partially purified tRNA (10 mg) was then loaded onto a Vydac C4 semipreparative HPLC column (cat. no. 214TP1010) equilibrated in buffer RP1. A linear gradient to 100% buffer RP2 (10 mM sodium phosphate (pH 4.5) and 15% methanol) was established over 70 min at a flow rate of 4 mL/min. Fractions were collected every 0.5 min and analyzed for threonine acceptance as described above. The highest purity fractions (> 1500 pmol/A₂₆₀) were pooled and dialyzed against buffer DT (2 mM HEPES (pH 7.0), 10 mM KCl) for storage.

Mutagenesis, Overexpression, and Purification of *E. coli* Threonyl-tRNA Synthetase (ThrRS_{EC}). A plasmid (pH8GW-ecThrRS) coding for an N-terminal polyhistidine fusion protein of WT ThrRS_{EC} was used for overexpression (21). ThrRS_{EC} mutants were generated from the plasmid using Quickchange mutagenesis methodology (Stratagene, La Jolla, CA) and from sets of complementary synthetic primers. The

entire ORF of each mutant was analyzed by DNA sequencing.

Expression of ThrRS_{Ec} was conducted as described previously (21). The length of induction was increased to 14 h to ensure complete repression of the endogenous ThrRS_{Ec} expression. Cell pellets from 4 L of culture (LB-kanamycin, 50 µg/mL) were collected by centrifugation (6000g, 15 min) resuspended in 100 mL of PL buffer (Tris-HCl (pH 8.0), 100 mM KCl, 0.1% β-mercaptoethanol, protease inhibitor cocktail (Roche Diagnostics Corp., Indianapolis, IA), 10 mM imidazole, and 0.1% Triton-X100). Cells were lysed by sonication and then centrifuged (25 000g, 45 min) to remove insoluble debris. The cleared lysate was applied to a 5 mL column of Ni-NTA resin (Qiagen, Valencia, CA). The column was washed with 15 volumes of PW buffer (Tris-HCl (pH 8.0), 100 mM KCl, 0.1% β-mercaptoethanol, protease inhibitor cocktail, and 10 mL of imidazole). Bound protein was eluted with 20 mL of PE buffer (Tris-HCl (pH 8.0), 20 mM KCl, 0.1% β-mercaptoethanol, and 200 mM imidazole). The eluate was concentrated to 5 mL using Centrprep-30 spin columns (Amicon, Beverly, MA) and dialyzed against 4 L of HP buffer (20 mM Tris-HCl (pH 7.5), 10 mM NaCl, and 0.1% β-mercaptoethanol). ThrRS_{Ec} was loaded onto a MonoQ HR 10/10 (Amersham Biosciences Corp., Piscataway, NJ) equilibrated in HP buffer. The column was developed using a linear salt gradient (0–0.6 M NaCl) over 60 min at a flow rate of 3 mL/min. Fractions containing ThrRS_{Ec} were collected and analyzed for purity by SDS PAGE. Fractions containing ultrapure proteins (>99%, judged by coomassie blue staining) were combined and dialyzed against PS buffer (15 mM HEPES (pH 7.0), 100 mM KCl, 5% glycerol (v/v), and 2 mM dithiothreitol). Dialyzed samples were then concentrated to >30 mg/mL, snap-frozen in liquid nitrogen, and stored at –80 °C. Enzyme concentration was determined by active-site titration (32). ThrRS_{Ec} point mutants were expressed and purified in the same manner. Native, untagged ThrRS_{Ec} was purified as described previously (33).

Purification of Aminoacylated tRNA^{Thr}. Purified tRNA^{Thr} was misacylated using an editing-deficient point mutant of ThrRS_{Ec} (H73A). Best results were obtained by incubating 2.9 µM ThrRS_{Ec}H73A with 30–40 µM tRNA^{Thr} and 200 µM [³H]serine (~1300 cpm/pmol) in aminoacylation buffer AT (50 mM HEPES (pH 7.0), 60 mM KCl, 10 mM MgCl₂, 2 mM ATP, 1 mM DTT, and 2 units of pyrophosphatase) for 20 min at 27 °C. Reaction progress was monitored using a filter binding assay (under these conditions serine acceptance for tRNA^{Thr} was nearly 1300 pmol/A₂₆₀) (34). The reaction was quenched with 0.1 volumes of 4 M sodium acetate (pH 4.3) and 1.1 volumes of water-saturated phenol. Following extraction of the aqueous phase, tRNA was precipitated with 0.4 volumes of isopropyl alcohol. The precipitate was washed with ethanol and resuspended in 10 mM sodium acetate. The aminoacylated tRNA was desalted using a Sephadex G-25 column equilibrated in 10 mM sodium acetate (pH 4.3). Desalted sample was then concentrated to >100 µM using a Centrprep-10 spin column, frozen in liquid nitrogen, and stored at –80 °C.

Aminoacylation and Substrate Dependence. The tRNA-charging reaction (100 µL) contained 50 mM HEPES (pH 7.5), 2 mM ATP, 10 mM MgCl₂, 200 µM serine, 30 µM [³H]serine (80 Ci/mol supplied by Amersham Biosciences),

and *E. coli* tRNA^{Thr} (0.03–2 µM). The mixture was equilibrated at 27 °C before the addition of ThrRS (100 pM). Reaction aliquots (10 µL) were removed at predetermined time intervals and mixed with 200 µL of 10% (w/v) trichloroacetic acid (TCA). Aminoacylated tRNA was isolated and quantified as described previously. Kinetic parameters were determined using initial rate methodology. *K_m* and *k_{cat}* values were derived from iterative nonlinear fitting of the theoretical Michaelis–Menten equation to the experimental values using the Levenberg–Marquardt algorithm (35).

Steady-State Deacylation Reactions. Deacylation assays (200 µL) were conducted at 27 °C in 20 mM Hepes (pH 7.5), 50 mM KCl, 2 mM MgCl₂, 2 µM Ser-tRNA^{Thr}, and catalytic amounts ThrRS (2–20 nM). Reactions were initiated with the addition of enzyme. At set time points, aliquots (36 µL) were precipitated with 200 µL of TCA (10% w/v). A portion of the filtrate (100 µL) was then removed and mixed with scintillation fluid. Free [³H]serine was quantified by liquid scintillation counting. The spontaneous hydrolysis rate of Ser-tRNA^{Thr} was measured similarly, but in the absence of enzyme. Total editing assays were performed as described previously (36). Radiolabel products (AMP) and intermediates (AA-AMP) were separated using thin-layer chromatography and visualized by phosphor imaging (37).

Transient-State Kinetics: Single-Turnover Studies. A Kintek RQF-3 rapid quench–flow apparatus (Kintek Corp., Austin, TX) was used for all transient-state kinetic experiments. The RQF-3 allows precise mixing of reagents and quenching of reaction mixtures on a 2 ms–2 m time scale. Reagents are loaded into separate sample loops (A and B) prior to mixing. Under the control of a computer-driven step motor, the samples (~26 µL total) are mixed in reaction loops of variable size and then quenched with a constant volume (95.5 µL) of 10% TCA. Reaction length is determined by a combination of flow rate and reaction loop length. These properties vary slightly between machines and were therefore calibrated as described previously (38).

For single-turnover deacylation assays, a solution was loaded into sample loop A consisting of ThrRS (30–60 µM) in 2× TMA buffer (200 mM Tris, 100 mM MES, 100 mM acetic acid, pH = 7.5) containing 2 mM MgCl₂ and 60 mM KCl and into sample loop B was loaded 2 µM [³H]Ser-tRNA^{Thr} (~1300 cpm/pmol) in a solution of 2 mM potassium acetate (pH 4.3), 2 mM MgCl₂, and 60 mM KCl. All experiments were performed at 27 °C. Reagents were then mixed, incubated for various lengths of time, and quenched. A portion (100 µL) of each quenched reaction was mixed with an equal volume of 5% TCA containing 100 mM serine and 50 µg/mL bovine serum albumin (BSA) in separate wells of a MultiScreen HTS filter plate (Millipore). Liberated amino acid was quantified by combining 150 µL of filtrate with 4 mL of Ecolite scintillation fluid (ICN) and counting on the wide channel of a Beckman LS 6500 (Beckman-Coulter, Fullerton, CA). Control experiments were performed to quantify recovery of free amino acid and retention of Ser-tRNA^{Thr} on the filter. Calibration of Ser-tRNA^{Thr} retention was performed as described above but in the absence of ThrRS. Background was low, indicating that >98% of Ser-tRNA^{Thr} was retained on the filter. Free amino acid recovery was measured similarly with [³H]serine rather than with the

Table 1

(a) tRNA ^{Thr} Expression and Purification			
enrichment step	threonine acceptance (pmol/A ₂₆₀ unit)	tRNA ^{Thr} (nmoles/0.7 L)	% yield (tRNA ^{Thr}) ^a
acid-phenol extraction (uninduced)	30 ± 3		
acid-phenol extraction (induced)	348 ± 75	42.5 ± 9.1	100 ^b
anion exchange	1368 ± 50	35.1 ± 1.3	83
RPHPLC	1663 ± 69	27.8 ± 1.1	79
(b) Kinetic Parameters for wt ThrES			
	<i>k</i> _{cat} (s ⁻¹)	<i>K</i> _m (μM)	<i>k</i> _{cat} / <i>K</i> _m (s ⁻¹ μM ⁻¹)
tRNA ^{Thr} (purified)	0.31 ± 0.01	0.06 ± 0.01	5.34

^a May include more than one isoform of tRNA^{Thr}. ^b Starting point for quantitation; cell lysate was not analyzed for threonine acceptance activity.

acylated substrate. Recoveries were reaction-loop-dependent and ranged from 57.9% ± 5.2% to 66.9% ± 3.8%.

Recombinant ThrRS used in this study was not previously characterized (21). Because the N-terminal-appended affinity tag could compromise catalysis, native enzyme was isolated for comparison. The two enzyme forms showed similar hydrolysis rate, demonstrating that the tag does not influence editing activity.

Solvent Isotope Experiments. All solutions were prepared in 99.9% deuterium oxide (Sigma). The final pD was determined by applying a correction factor (ΔpH) to the readings from a standard glass electrode according to the deuterium atom fraction (*n*) (39). The correction factor was determined using the equation ΔpH = pD - meter reading = (0.173*n*² + 0.221*n*). A pL = 8.5 (where rates were independent of pH/pD) was used in experiments where H₂O/D₂O ratios were varied. pH measurements were made at 27 °C.

pH Dependence of Ser-tRNA^{Thr} Hydrolysis. Reactions were performed in a Kintek RQF-3 as described above with minor changes. At low pH (<6.0) [³H]Ser-tRNA^{Thr} was combined with the 2× buffering agent (TMA (200 mM Tris, 100 mM MES, 100 mM acetic acid, 2 mM MgCl₂, 60 mM KCl)) and the enzyme with dilute buffer (2.5 mM HEPES (pH 7.0), 2 mM MgCl₂, 60 mM KCl). A constant ionic strength (*I* = 0.308 M) was maintained. The final pH of each reaction was determined from direct measurement of mock reactions. Enzyme stability was analyzed as follows. ThrRS (21 μM) was mixed manually with appropriate buffer (pH 4.5–9.0, 40 μL volume) and incubated for 1 min. A 10 μL aliquot was diluted 10-fold with 500 mM HEPES (pH 7.5)/60 mM KCl. Finally, the enzyme was diluted to 20 nM in deacylation buffer (50 mM HEPES (pH 7.5), 60 mM KCl, 2 mM MgCl₂, and 2 μM Ser-tRNA^{Thr}) and analyzed for activity. The activity was similar across the full pH range, showing that the enzyme was stable, over the course of a typical single-turnover reaction.

Because the uncatalyzed hydrolysis of Ser-tRNA^{Thr} was also pH-dependent, hydrolysis rates were determined in the absence of ThrRS. As expected, the data was described by a rate law determined for other aminoacyl-tRNAs under similar conditions (37 °C, *I* = 0.3). A p*K*_a = 7.87 ± 0.1 was obtained for the α-amino group of ligated serine, and a

rate of spontaneous hydrolysis of 0.026 min⁻¹ at pH 9.0 was determined (40). This control experiment served two purposes: to establish background hydrolysis rates for and to measure the p*K*_a of the substrate's ionizable α-amino group in the TMA buffer system. This value was in agreement with those published for several other aminoacyl-tRNAs (p*K*_a = 7.8) determined at 37 °C and *I* = 0.3, and thus provided data for background subtraction.

Data Analysis. Time courses for single-turnover hydrolysis assays were fit to a first-order single-exponential equation (eq 1) in Kaleidagraph data analysis software (Synergy Software, Reading, PA), where [P]_{total} and [P] are the concentrations of tRNA^{Thr}-bound and free serine and *k*_{obs} is the observed rate constant. For pH-rate data, *k*_{obs} was plotted as a function of pH/pD and fit to eq 2, where *k*_b is the first-order rate constant for amino acid hydrolysis by ThrRS.

Equations:

$$\frac{[P]}{[P]_{\text{total}}} = (1 - e^{-k_1 t}) \quad (1)$$

$$k_{\text{obs}} = \frac{k_b}{1 + (10^{(pK_a - \text{pH})})} + k_{\text{uncat}}$$

$$\text{and } k_{\text{obs}} = k_{\text{cat}}[\text{ES}]/[\text{E}]_0$$

$$\text{where } [\text{ES}]/[\text{E}]_0 = \{E_0 + S_0 + K_d - (E_0 + S_0 + K_d)^2 - 4E_0S_0\}/2E_0; \quad [\text{E}]_0 = [\text{E}] + [\text{ES}]$$

$$\text{and } [\text{S}]_0 = [\text{S}] + [\text{ES}] \quad (2)$$

RESULTS

Production of Substrate for Editing. Milligram quantities of tRNA^{Thr} were required for mechanistic studies. Although quantities of this magnitude can be generated by in vitro transcription, a system to produce the needed tRNA^{Thr} in vivo was designed. The rationale was that an efficient production system in vivo would in principle bypass the difficulties of isolating large scale amounts of homogeneous tRNA^{Thr} from a reaction run in vitro, where products with *N* - 1 or *N* + 1 nucleotides will appear (41).

An oligonucleotide cassette was constructed by inserting the gene for *E. coli* tRNA^{Thr} (*thrW*) into plasmid pEXT-20. Sixty-four nucleotides of flanking genomic sequence (20 upstream and 44 downstream nucleotides) were included to allow for post-transcriptional processing and maturation. The construct was introduced into MRE600 cells and expression induced with IPTG (pTac promoter). A crude preparation of total tRNA from these cells was enriched ~10-fold for threonine acceptance activity, thus demonstrating a significant overexpression of tRNA^{Thr} (Table 1). Threonine-specific tRNA was resolved from the other contaminating tRNAs by anion exchange chromatography (DNAPAC-100), followed by reversed-phase HPLC. The resulting preparation had 1663 ± 69 pmol of threonine acceptance/A₂₆₀, which gives a purity of essentially 100%. The kinetic properties of purified tRNA^{Thr} (*k*_{cat} = 0.31 ± 0.01 s⁻¹, *K*_m = 0.06 ± 0.01 μM) were consistent with those reported previously for native tRNA^{Thr} (30).

Single-Turnover Hydrolysis of Misacylated tRNA^{Thr}. To understand the underlying mechanism of the chemical step of the editing reaction, we first concentrated on developing a reliable assay for single-turnover kinetics. To start, ThrRS

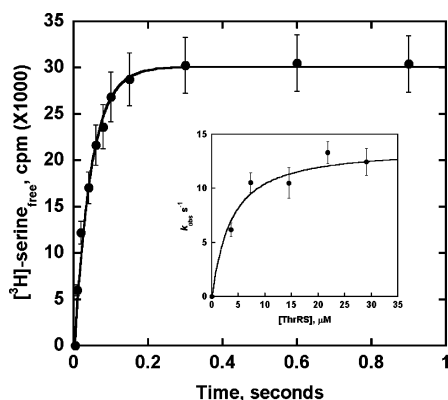


FIGURE 1: Deacylation of Ser-tRNA^{Thr}. ThrRS-catalyzed single-turnover deacylation of [³H]Ser-tRNA^{Thr}, pH = 7.5, 2 mM MgCl₂, and 60 mM KCl. Inset: deacylation rates (Ser-tRNA^{Thr} = 1 μM) were determined at various concentrations of ThrRS (2–30 μM). Data were fit as described in Materials and Methods.

was incubated with Mg-ATP and serine to produce misactivated seryl-adenylate and pyrophosphate (Scheme 1A). In the absence of tRNA^{Thr}, Ser-AMP was slowly hydrolyzed ($0.0001 \pm 0.0001 \text{ s}^{-1}$) to AMP and serine. However, addition of catalytic amounts of tRNA resulted in rapid ATP hydrolysis by iterative cycles of serine misactivation, transfer to tRNA, and clearance (36, 42). Because of the high background from the competing, uncatalyzed reaction with hydroxide (40), accurate steady-state rate measurements for the half-reaction (hydrolysis of Ser-tRNA^{Thr}) proved difficult.

In contrast, rapid-kinetic analysis of the half-reaction gave reproducible rate data. These experiments were performed by mixing ThrRS (21.8 μM) with [³H]Ser-tRNA^{Thr} (1 μM), using a RQF-3 rapid quench-flow apparatus. Reaction progress was monitored by detection of free [³H]serine at various time intervals. Because the concentration of ThrRS was in excess of [³H]Ser-tRNA^{Thr}, only a single turnover was observed. Time course data from these experiments were well fit with a single-exponential equation (eq 1) that took into account the background hydrolysis rate (Figure 1). Doubling the concentration of enzyme from 15 to 30 μM had little effect on k_{cat} . Thus, enzyme-substrate association did not limit k_{cat} so that, under these circumstances, greater than 90% of the substrate was bound by ThrRS. This analysis provided the conditions for us to move forward with a more detailed analysis of the chemical step.

pH-Rate Dependence of Post-Transfer Editing. To explore the role of ionizable groups in the chemical step of ThrRS-catalyzed hydrolysis of Ser-tRNA^{Thr}, the reaction was studied as a function of pH (4.5–9.0). Under the established single-turnover conditions, k_{obs} showed a log-linear dependence on pH (Figure 2). The data is described by eq 2, with an enzymatic reaction rate ($k_{\text{cat}}(\text{H}_2\text{O}) = 22.5 \pm 0.8 \text{ s}^{-1}$) that is governed by a single, apparent ionization pK_a (7.27 ± 0.06). Over the entire range of pH 4.5–9.0, rates were independent of enzyme concentration (ThrRS $\geq 21.5 \text{ μM}$). In separate controls, uncatalyzed hydrolysis rates were measured at each pH (data not shown) to determine the apparent pK_a of the seryl α-amino group that is known to influence spontaneous hydrolysis. Our data matched that of a previous study and was used to determine the ionization constant for the seryl α-amino moiety as $\text{pK}_a = 7.87 \pm 0.1$ (40).

Solvent Isotope Effects Strongly Influence ThrRS-Catalyzed Editing. Solvent isotope studies can determine the role of

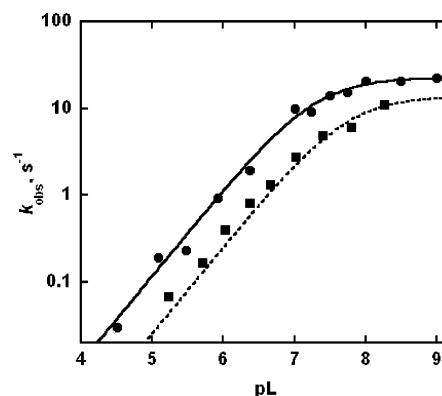


FIGURE 2: The pH/pD-dependent deacylation of Ser-tRNA^{Thr}. [³H]-Ser-tRNA^{Thr} deacylation rates were measured over the pL range of 4.5–9.0, in the presence of ThrRS (21.5 μM), 2 mM MgCl₂, and 60 mM KCl. Reactions were conducted in H₂O (circles) or D₂O (squares). The data were fit to eq 2.

proton transfers in chemical reactions (43). With this in mind, the ThrRS-dependent clearance of Ser-tRNA^{Thr} was investigated in solvent with high deuterium oxide content (D₂O = 95%) over a range of pD values (4.5–9.0). Like the complementary profile in H₂O, rate data was described by eq 2 and gave $\text{pK}_a = 7.73 \pm 0.06$. Thus D₂O sharply shifted the apparent pK_a ($\Delta\text{pK}_a = \sim 0.5$). In addition, $k_{\text{cat}}(\text{D}_2\text{O}^{95}) = 13.6 \pm 0.5 \text{ s}^{-1}$ was substantially reduced, with $k_{\text{cat}}(\text{H}_2\text{O})/k_{\text{cat}}(\text{D}_2\text{O}) = \sim 1.7$. These results suggest that proton transfer is at the heart of the chemical step for editing.

Aware that interpretation of a kinetic solvent isotope effect (KSIE) can be less than straightforward when protein structural integrity is compromised by proton exchange or differences in solvent properties, control experiments attempted to detect changes in ThrRS that could indirectly affect the chemical step (44). The first experiment was designed to identify activity changes resulting from extensive hydrogen/deuterium exchange at peptide bonds and protein side chains at slowly exchanging sites ($t_{1/2} > 30 \text{ min}$). In this experiment, ThrRS was dialyzed against and stored in buffer with high deuterium oxide content (99%). Single-turnover experiments (in 3% D₂O) were then used to compare activities of enzymes stored in H₂O and D₂O, before the backbone side-chain hydrogens (or deuteriums) were exchanged out. Rate measurements produced the same values as obtained for the “unexchanged” enzyme (data not shown), suggesting that the observed KSIE was not an incidental consequence of massive deuterium incorporation into the protein.

In a second experiment, the rate of steady-state deacylation (Ser-tRNA^{Thr}, 1 μM; ThrRS, 3 nM) was measured at a rate-insensitive pL = 8.5 and in solvents of high or low D₂O content. Rates were independent ($k_{\text{obs}}(\text{H}_2\text{O}) = 2.4 \pm 0.2 \text{ s}^{-1}$ and $k_{\text{obs}}(\text{D}_2\text{O}^{95}) = 2.3 \pm 0.2 \text{ s}^{-1}$) of D₂O content. Under these conditions, Ser-tRNA^{Thr} hydrolysis was slower and presumed to be limited by one or more nonchemical steps. The identical k_{obs} under the two different conditions is also consistent with no perturbation of the enzyme structure by deuterium.

Mutational Analysis of the Pocket for Editing. Having established the prominence of a ionizable group(s) as essential for the chemical step, we sought to determine which of those known to be in the pocket for editing were needed for proton transfer. For this purpose, a multiple sequence alignment of known ThrRS, AlaRS, and AlaXp editing

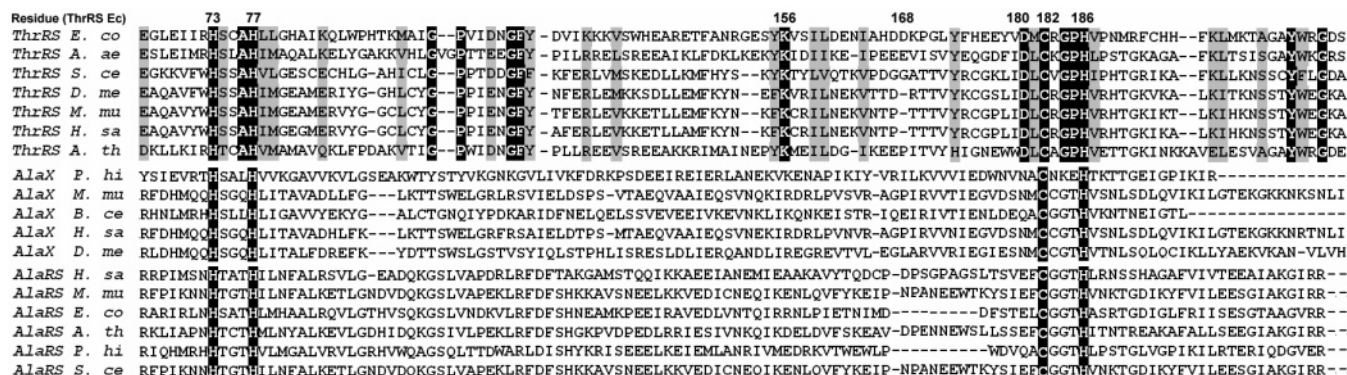


FIGURE 3: Multiple sequence alignment of class II editing domains (ED_{CIIa}). Identical residues are highlighted in black. Similar residues (gray) are highlighted for ThrRS sequences only. Residues, mutated in this study, are numbered (*E. coli* sequence).

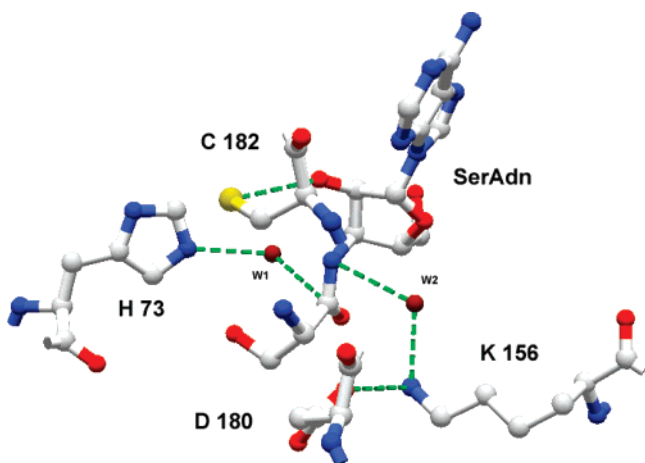


FIGURE 4: ThrRS editing active site with SerAdn. Hydrogen bonds are shown in green, and water molecules are in deep red. Coordinates are derived from Dock-Bregeon et al.

domains was constructed. This alignment revealed many conserved residues (Figure 3). These residues were mapped to a structure (of the ThrRS editing domain) that had been solved in the presence of the post-transfer editing substrate analogue 3-amino-3-deoxy(seryl)adenosine (SerAdn) (29). Seven conserved residues in the putative ligand binding pocket and active site (H73, H77, K156, D168, D180, C182, H186) were selected for mutagenesis and are marked in Figure 3 (also shown in Figure 4). Each mutant enzyme was analyzed for activity for Ser-tRNA^{Thr} hydrolysis. In addition, misacylation of tRNA^{Thr} mischarging rates (with serine) was studied under standard aminoacylation conditions (Table 2).

Four of the residues selected for mutagenesis are conserved through evolution in both ThrRS, AlaRS, and the editing-proficient natural fragment known as AlaXp. These four residues are part of two motifs (H₇₃XXXH₇₇ and C₁₈₂-XXXH₁₈₆, in *E. coli* ThrRS). Their spatial arrangement, relative to the reactive carbonyl center of aminoacyl-A₇₆, is known from a structure of the editing domain bound with substrate analogue (SerAdn) (29). H73 is positioned to hydrogen bond to a water molecule located 2.9 Å away from and perpendicular to the plane of the reactive carbonyl center. H77 sterically defines the aminoacyl-adenosine binding pocket and is proposed to block editing of threonylated tRNA^{Thr}. H186 hydrogen bonds to C182, which in turn is coordinated to the 2'-hydroxyl of SerAdn.

As for the other residues, D168 is H-bonded to the exocyclic ring nitrogen of A₇₆ of bound tRNA^{Thr}. In the SerAdn-bound

Table 2: Kinetic Parameters for Ec ThrRS Variants

ThrRS	k_{cat}^{obs} (deacylation rate) $s^{-1} a$	k_a^{obs} (misacylation rate) $s^{-1} b$	KSIE $k_b(H_2O)/k_b(D_2O)^c$
none	0.0002 ± 0.0001		
WT	21.0 ± 2.0	n.d.	1.7
H73A ^d	0.0029 ± 0.0006	0.24 ± 0.05	
H73N ^d	0.0024 ± 0.0004		
H77A ^d	0.24 ± 0.01	0.22 ± 0.02	1.0
K156A	0.18 ± 0.02	0.21 ± 0.03	1.1
K156D	0.12 ± 0.02		
D168A	22.0 ± 1.2	n.d.	
D180A	0.42 ± 0.01	0.17 ± 0.07	
D180N	0.47 ± 0.05		
C182A ^d	0.016 ± 0.001	0.22 ± 0.03	
C182S ^d	0.035 ± 0.001	0.25 ± 0.02	
H186A ^d	0.32 ± 0.04	0.19 ± 0.01	1.0

^a Measured under single-turnover conditions: 23 μM ThrRS and 1 μM Ser-tRNA^{Thr} in 1× TMA (pH 7.5) containing 60 mM KCl and 10 mM MgCl₂. ^b Determined by steady-state measurements: 3 nM ThrRS, 1 μM tRNA^{Thr}, 2 mM ATP, 1 mM [³H]serine, 1× TMA (pH 7.5), 60 mM KCl, and 10 mM MgCl₂. ^c Single-turnover deacylation rates were measured at pL = 8.5 in H₂O and 95% D₂O. The KSIE is calculated as the ratio of the rates. ^d Conserved among eukaryotic/bacterial ThrRSs and AlaRSs.

structure, K156 interacts with a water molecule in the editing domain active site. The water is within hydrogen-bonding distance of the nitrogen of the substrate analogue amide linker. This amide is replaced by oxygen in the true substrate (aminoacyl-tRNA esters) and corresponds to the leaving group (ribose 3' hydroxyl) of the hydrolysis reaction. K156, in its protonated form, was proposed to stabilize leaving group departure via a proton-transfer mechanism with water (29). Finally, D180 is located in proximity (~3 Å) to the ε-nitrogen of K156 and the α-amino moiety of SerAdn. Because D180 and the α-amino moiety of serine should exhibit charge complementarity at physiological pH, it follows that D180 might use electrostatic interactions to position seryl-A₇₆ for hydrolysis.

Ten of the individual substitutions, including the aforementioned widely conserved three histidines and single cysteine, resulted in a significant (> 10-fold) decrease in the rate of enzyme-catalyzed hydrolysis and in an increase in mischarging. The exception was the Ala substitution of D168, where the D168A ThrRS had the same k_{cat} as the wild-type enzyme. The reduction in k_{cat} was largest (10^{3.9}-fold) for H73A ThrRS, which had a rate slightly above that of the uncatalyzed reaction. More conservative substitutions at

position H73 (D, E, N, and Q; Table 2 and data not shown) did not improve activity. This result is consistent with H73 providing the critical proton abstraction associated with $pK = 7.27$, in the chemical step of the deacylation reaction.

The next most dramatic effect was seen with Ala and Ser substitutions of C182. Here the rate diminishment was about 10-fold less than that seen with substitutions of H73. C182 is proposed to participate in a tether that holds the 2'-OH of the substrate for deacylation in the site for editing. This tether is stabilized by bonding of H186 to C182. The 60–70-fold rate reduction seen with the H186A substitution is supportive of this model.

With residues that tolerated substitutions without virtual elimination of activity, the residual activity was sufficient to measure kinetic isotope effects. For H77A, K156A, and H186A ThrRS, single-turnover measurements were performed in H_2O and D_2O^{95} ($pL = 8.5$). In contrast to the wild-type enzyme, none of these variants had a significant KSIE (Table 2).

Chemical Rescue Experiments. Several attempts were made to rescue the activity of the histidine mutants H73A, H73G, H77A, and H186A with exogenous amines. Deacylation reactions ($pH\ 8.0$) were supplemented with imidazole, imidazole analogues, and other small molecule amines, at concentrations up to 500 mM (solubility permitting). None of these molecules significantly enhanced the activity of these mutants toward Ser-tRNA^{Thr}.

DISCUSSION

Class II AARSs are known to form a productive binary complex by a two-step mechanism: diffusion-controlled association followed by a conformational transition (45, 46). Under single-turnover conditions used here, the association of Ser-tRNA^{Thr} with ThrRS does not contribute to the observed hydrolysis rate. Several lines of evidence suggest that product formation, and not the conformational change, limits the observed rate. Specifically, the transition was reported by others, for another class II enzyme (PheRS), to be fast ($600\ s^{-1}$ and rapidly reversible), compared to the maximal hydrolysis rate seen here ($22.5\ s^{-1}$). The forward rate (k_2) of the conformational transition in that study decreased with increasing pH. In contrast, our studies showed a clear increase in ThrRS activity with pH, and a significant KSIE ($k_{cat}(H_2O)/k_{cat}(D_2O) = 1.7$) was observed. Taken together, these data are consistent with direct measurement of Ser-tRNA^{Thr} ester bond cleavage (product formation) on the enzyme (47).

With this perspective, a simple model for mischarged substrate binding and catalysis is shown in Figure 5. The first step involves formation of a binary complex (K_b). The complex is formed using identity elements within the tRNA body and complementary residues on the surface of ThrRS. In the model, binding of the 3'-end of tRNA to the editing active site is represented as a reversible conformational (tRNA) change of the CCA end (K_t) driven by binding of Ser-A₇₆. Once established, these interactions position the aminoacyl-A₇₆ head group for catalysis (k_{chem}). In the model, negative changes in the recognition of the aminoacyl-A₇₆ moiety (e.g., mutations) shift the equilibrium (K_t) toward the initial, inactive binary complex. Under circumstances where the complex is maintained (single-turnover conditions) the

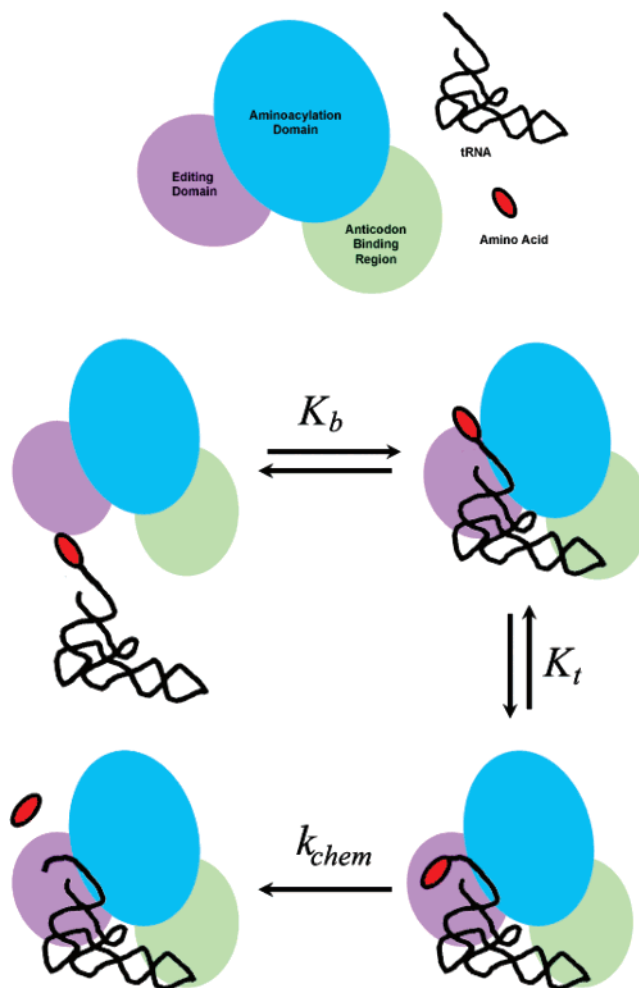


FIGURE 5: Possible mechanism for editing by ThrRS. Protein–RNA interactions, or identity elements, drive formation of the “inactive” binary complex (K_b , depicted as a single step for simplicity). The terminal adenosine (A₇₆) and attached amino acid (red oval) are brought in proximity to the editing active site, where they may bind (K_t). Once bound, the aminoacyl–tRNA is positioned for irreversible hydrolysis (k_{chem}).

hydrolysis rate is determined by the fraction of molecules in the active conformation. When the fraction is severely reduced by mutation, k_{cat} no longer represents the chemical step (k_{chem}). The lack of a KSIE for several of the active-site mutants is consistent with the above model. In, particular, mutation of sites constituting aminoacyl-A₇₆ binding interactions could shift K_t toward the inactive complex and change the rate-determining step.

Hydrolysis was stimulated by an ionization with an apparent $pK_a = 7.27$. In deuterium oxide (95% D_2O), the rate profile appeared similar but with an upward apparent pK_a shift ($\Delta pK_a \approx 0.5$ units) and decrease in maximum rate ($k_{cat}(H_2O)/k_{cat}(D_2O) \approx 1.7$ -fold). Isotopic pK_a shifts of this magnitude are common for solvent-exposed amino groups involved in proton-transfer reactions (43). The accompanying k_{cat} decrease is indicative of a mechanism involving transition-state proton transfer. Chemical models of ester hydrolysis showed that a KSIE of 1.9 for imidazole-catalyzed hydrolysis of *N,O*-diacetylserinamide (48). The pH-rate and solvent isotope studies seen here demonstrate that side-chain ionization and transition-state proton transfer are significant to the ThrRS-mediated breakdown of misacylated tRNAs, consistent with general acid/base catalysis.

In agreement with previous studies, editing defective mutants efficiently mischarged tRNA^{Thr} with serine (Table 2; k_a) (14, 29). Three histidines ($pK_{a \text{ Expected}} = 6.9$) important for activity are found in the signature sequence motif (**H**₇₃-XXX-**H**₇₇ and **C**₁₈₂-XXX-**H**₁₈₆)² of the ED_{CIIa} and are conserved among all ThrRSs(N2), AlaRSs, and AlaXps. H73 is optimally positioned to function as a general base by accepting a proton from water during catalysis. Chemical models of aminoacyl-tRNA breakdown show that imidazole acts as a general acid-base when leaving groups are poor ($pK_a \geq 12.5$). Significantly, the 3' hydroxyl of adenosine has a pK_a of ~ 12.5 (49–51). Substitution of H73 to alanine or asparagine reduced the single-turnover hydrolysis rate essentially to the limits of our detection ($\sim 10^4$ -fold reduction). This substitution of H₇₃ had by far the most profound effect, and that observation, together with supporting data, make a strong case for the imidazole side chain of H73 acting as a general acid-base during hydrolysis.

Alanine substitution of D180 (D180A ThrRS) reduced the single-turnover hydrolysis rate ~ 50 -fold. AlaXp of *Pyrococcus hirokoshii* (AlaX_{ph}) has an asparagine at the analogous position. Because AlaX_{ph} efficiently hydrolyzes Ser-tRNA^{Ala}, the asparagine mutant (D180N ThrRS) might be expected to recover some of the hydrolytic activity lost on substitution of D for A (23). However, the conservative substitution did not improve activity. Because the aspartate side chain is required for efficient editing, its ability to ionize may promote activity by positioning another important residue, K156. Interestingly, D180 is found in all sequenced ThrRS N2-editing domains but is absent in AlaRSs and AlaXps. In addition to the asparagine found in *P. hirokoshii* AlaXp, glutamine and glutamate are found at analogous positions of AlaRSs and AlaXps.²

Mutation of K156 to alanine decreases single-turnover hydrolysis of Ser-tRNA^{Thr} by ~ 200 -fold. In the structure of ThrRS, with bound SerAdn, K156 interacts with both D180 and a water molecule. The water hydrogen bonds to nitrogen of the substrate analogue's amide linker. This amide is replaced by oxygen in the true substrate (aa-tRNA esters) and represents the leaving group (ribose 3' hydroxyl) of the hydrolysis reaction. K156, in its protonated form, was proposed to stabilize leaving group departure via a proton-transfer mechanism with water (29). In our studies, the pH-rate profile revealed only a single ionization constant. However, rate measurements at pH > 9 were not possible. Thus, a role for K156 in catalysis is still possible in principle.

Interestingly, despite contacts with the exocyclic amine of A₇₆, D168 plays no apparent role. Substitution with alanine had no effect on the single-turnover hydrolysis rate, and ThrRS D168A was unable to produce measurable quantities of serylated tRNA.

The role of other active-site residues (H77, H186, C182) is unclear. For example, C182 interacts with the 2'-hydroxyl of SerA₇₆. From this position, C182 is unlikely to directly influence bond formation/breaking. However, the C182A (or C182S) mutation profoundly diminished k_{cat} ($\sim 10^3$ -fold). The decrease cannot be explained by disruption of the binary complex because the complex is maintained under the experimental conditions. Furthermore, because the apo and

SerAdn-bound forms of the enzyme lack appreciable differences in side-chain positioning, it is unlikely that mutation of C182 to Ala prevents substrate-induced reorganization of the editing active site (induced-fit mechanism). Instead, the role of C182, as well as of H186 and H77, may be to provide local binding contacts to the substrate aminoacyl-A₇₆ head group. Indeed, through interactions with the 2'-hydroxyl, C182 appears to position the flexible 3'-aminoacyl-CCA within the editing active site and to stabilize the C2'-endo conformation of ribose (29).

Alanine substitution of any of four residues (**H**₇₃-XXX-**H**₇₇ and **C**₁₈₂-XXX-**H**₁₈₆) conserved across all reported sequences of ThrRS, AlaRS, and AlaXp resulted in a greater than 50-fold reduction in k_{cat} , with virtual abolishment of activity when H₇₃ was substituted. A less than 2-fold reduction in editing activity of AlaRS led to neurodegeneration and ataxia in the mouse. Thus, reductions in activity of the magnitude seen here would doubtless be lethal. Indeed, the mutation in AlaRS that led to disease in the mouse was the nonconserved alanine (4). Thus, the results also illustrate how, at the molecular level, disease and probably lethality can come down to disruption of a single proton-transfer event, such as the one dependent on H₇₃.

REFERENCES

1. Nangle, L. A., De Crecy Lagard, V., Doring, V., and Schimmel, P. (2002) Genetic code ambiguity. Cell viability related to the severity of editing defects in mutant tRNA synthetases, *J. Biol. Chem.* 277, 45729–45733.
2. Doring, V., Mootz, H. D., Nangle, L. A., Hendrickson, T. L., de Crecy-Lagard, V., Schimmel, P., and Marliere, P. (2001) Enlarging the amino acid set of *Escherichia coli* by infiltration of the valine coding pathway, *Science* 292, 501–504.
3. Nangle, L. A., Motta, C. M., and Schimmel, P. (2006) Global effects of mistranslation from an editing defect in mammalian cells, *Chem. Biol.* 13, 1091–1100.
4. Lee, J. W., Beebe, K., Nangle, L. A., Jang, J., Longo-Guess, C. M., Cook, S. A., Davisson, M. T., Sundberg, J. P., Schimmel, P., and Ackerman, S. L. (2006) Editing-defective tRNA synthetase causes protein misfolding and neurodegeneration, *Nature* 443, 50–55.
5. Pauling, L. (1958) *Festschr. Arthur Stoll*, 597.
6. Loftfield, R. B., and Vanderjagt, D. (1972) The frequency of errors in protein biosynthesis, *Biochem. J.* 128, 1353–1356.
7. Hendrickson, T. L., Nomanbhoy, T. K., de Crecy-Lagard, V., Fukai, S., Nureki, O., Yokoyama, S., and Schimmel, P. (2002) Mutational separation of two pathways for editing by a class I tRNA synthetase, *Mol. Cell* 9, 353–362.
8. Hendrickson, T. L., Nomanbhoy, T. K., and Schimmel, P. (2000) Errors from selective disruption of the editing center in a tRNA synthetase, *Biochemistry* 39, 8180–8186.
9. Eldred, E. W., and Schimmel, P. R. (1972) Rapid deacylation by isoleucyl transfer ribonucleic acid synthetase of isoleucine-specific transfer ribonucleic acid aminoacylated with valine, *J. Biol. Chem.* 247, 2961–2964.
10. Schmidt, E., and Schimmel, P. (1994) Mutational isolation of a sieve for editing in a transfer RNA synthetase, *Science* 264, 265–267.
11. Wong, F. C., Beuning, P. J., Silvers, C., and Musier-Forsyth, K. (2003) An isolated class II aminoacyl-tRNA synthetase insertion domain is functional in amino acid editing, *J. Biol. Chem.* 278, 52857–52864.
12. Larkin, D. C., Williams, A. M., Martinis, S. A., and Fox, G. E. (2002) Identification of essential domains for *Escherichia coli* tRNA(Leu) aminoacylation and amino acid editing using minimalist RNA molecules, *Nucleic Acids Res.* 30, 2103–2113.
13. Lincecum, T. L., Jr., Tkalalo, M., Yaremchuk, A., Mursinna, R. S., Williams, A. M., Sproat, B. S., Van Den Eynde, W., Link, A., Van Calenbergh, S., Grotli, M., Martinis, S. A., and Cusack, S. (2003) Structural and mechanistic basis of pre- and posttransfer editing by leucyl-tRNA synthetase, *Mol. Cell* 11, 951–963.

² Based on structure and sequence alignments.

14. Dock-Bregeon, A., Sankaranarayanan, R., Romby, P., Caillet, J., Springer, M., Rees, B., Francklyn, C. S., Ehresmann, C., and Moras, D. (2000) Transfer RNA-mediated editing in threonyl-tRNA synthetase. The class II solution to the double discrimination problem, *Cell* 103, 877–884.
15. Sasaki, H. M., Sekine, S., Sengoku, T., Fukunaga, R., Hattori, M., Utsunomiya, Y., Kuroishi, C., Kuramitsu, S., Shirouzu, M., and Yokoyama, S. (2006) Structural and mutational studies of the amino acid-editing domain from archaeal/eukaryal phenylalanyl-tRNA synthetase, *Proc. Natl. Acad. Sci. U.S.A.* 103, 14744–14749.
16. Liu, Y., Liao, J., Zhu, B., Wang, E. D., and Ding, J. (2006) Crystal structures of the editing domain of *Escherichia coli* leucyl-tRNA synthetase and its complexes with Met and Ile reveal a lock-and-key mechanism for amino acid discrimination, *Biochem. J.* 394, 399–407.
17. Ishijima, J., Uchida, Y., Kuroishi, C., Tuzuki, C., Takahashi, N., Okazaki, N., Yutani, K., and Miyano, M. (2006) Crystal structure of alanyl-tRNA synthetase editing-domain homolog (PH0574) from a hyperthermophile, *Pyrococcus horikoshii* OT3 at 1.45 Å resolution, *Proteins* 62, 1133–1137.
18. Murayama, K., Kato-Murayama, M., Katsura, K., Uchikubo-Kamo, T., Yamaguchi-Hirafuji, M., Kawazoe, M., Akasaka, R., Hanawa-Suetsugu, K., Hori-Takemoto, C., Terada, T., Shirouzu, M., and Yokoyama, S. (2005) Structure of a putative trans-editing enzyme for prolyl-tRNA synthetase from *Aeropyrum pernix* K1 at 1.7 Å resolution, *Acta Crystallogr., Sect. F: Struct. Biol. Cryst. Commun.* 61, 26–29.
19. Fukunaga, R., and Yokoyama, S. (2005) Crystal structure of leucyl-tRNA synthetase from the archaeon *Pyrococcus horikoshii* reveals a novel editing domain orientation, *J. Mol. Biol.* 346, 57–71.
20. Fukunaga, R., Fukai, S., Ishitani, R., Nureki, O., and Yokoyama, S. (2004) Crystal structures of the CP1 domain from *Thermus thermophilus* isoleucyl-tRNA synthetase and its complex with L-valine, *J. Biol. Chem.* 279, 8396–8402.
21. Beebe, K., Merriman, E., Ribas De Pouplana, L., and Schimmel, P. (2004) A domain for editing by an archaeobacterial tRNA synthetase, *Proc. Natl. Acad. Sci. U.S.A.* 101, 5958–5963.
22. Cusack, S., Yaremchuk, A., and Tkalco, M. (2000) The 2 Å crystal structure of leucyl-tRNA synthetase and its complex with a leucyl-adenylate analogue, *EMBO J.* 19, 2351–2361.
23. Ahel, I., Korencic, D., Ibba, M., and Soll, D. (2003) Trans-editing of mischarged tRNAs, *Proc. Natl. Acad. Sci. U.S.A.* 100, 15422–15427.
24. Beuning, P. J., and Musier-Forsyth, K. (2000) Hydrolytic editing by a class II aminoacyl-tRNA synthetase, *Proc. Natl. Acad. Sci. U.S.A.* 97, 8916–8920.
25. Roy, H., Ling, J., Irnov, M., and Ibba, M. (2004) Post-transfer editing in vitro and in vivo by the beta subunit of phenylalanyl-tRNA synthetase, *EMBO J.* 23, 4639–4648.
26. Beebe, K., Ribas De Pouplana, L., and Schimmel, P. (2003) Elucidation of tRNA-dependent editing by a class II tRNA synthetase and significance for cell viability, *EMBO J.* 22, 668–675.
27. Schimmel, P., and Ribas de Pouplana, L. (2001) Formation of two classes of tRNA synthetases in relation to editing functions and genetic code, *Cold Spring Harbor Symp. Quant. Biol.* 66, 161–166.
28. Bovee, M. L., Pierce, M. A., and Francklyn, C. S. (2003) Induced fit and kinetic mechanism of adenylation catalyzed by *Escherichia coli* threonyl-tRNA synthetase, *Biochemistry* 42, 15102–15113.
29. Dock-Bregeon, A. C., Rees, B., Torres-Larios, A., Bey, G., Caillet, J., and Moras, D. (2004) Achieving error-free translation; the mechanism of proofreading of threonyl-tRNA synthetase at atomic resolution, *Mol. Cell* 16, 375–386.
30. Ruan, B., Bovee, M. L., Sacher, M., Stathopoulos, C., Poralla, K., Francklyn, C. S., and Soll, D. (2005) A unique hydrophobic cluster near the active site contributes to differences in borrelidin inhibition among threonyl-tRNA synthetases, *J. Biol. Chem.* 280, 571–577.
31. Hasegawa, T., Miyano, M., Himeno, H., Sano, Y., Kimura, K., and Shimizu, M. (1992) Identity determinants of *E. coli* threonine tRNA, *Biochem. Biophys. Res. Commun.* 184, 478–484.
32. Fersht, A. R., Ashford, J. S., Bruton, C. J., Jakes, R., Koch, G. L., and Hartley, B. S. (1975) Active site titration and aminoacyl adenylate binding stoichiometry of aminoacyl-tRNA synthetases, *Biochemistry* 14, 1–4.
33. Dignam, J. D., Rhodes, D. G., and Deutscher, M. P. (1980) Purification and structural characterization of rat liver threonyl transfer ribonucleic acid synthetase, *Biochemistry* 19, 4978–4984.
34. Buechter, D. D., and Schimmel, P. (1993) Dissection of a class II tRNA synthetase: determinants for minihelix recognition are tightly associated with domain for amino acid activation, *Biochemistry* 32, 5267–5272.
35. Cornish-Bowden, A. (1995) *Fundamentals of Enzyme Kinetics*, 2nd ed., pp 297–315, Portland Press Ltd.
36. Schreier, A. A., and Schimmel, P. R. (1972) Transfer ribonucleic acid synthetase catalyzed deacylation of aminoacyl transfer ribonucleic acid in the absence of adenosine monophosphate and pyrophosphate, *Biochemistry* 11, 1582–1589.
37. Khvorova, A., Motorin, Y., and Wolfson, A. D. (1999) Pyrophosphate mediates the effect of certain tRNA mutations on aminoacylation of yeast tRNA(Phe), *Nucleic Acids Res.* 27, 4451–4456.
38. Waas, W. F., Rainey, M. A., Szafranska, A. E., and Dalby, K. N. (2003) Two rate-limiting steps in the kinetic mechanism of the serine/threonine specific protein kinase ERK2: a case of fast phosphorylation followed by fast product release, *Biochemistry* 42, 12273–12286.
39. Schowen, K., and Schowen, R. (1982) Solvent isotope effects on enzyme systems, *Methods Enzymol.* 87, 551–606.
40. Wolfenden, R. (1963) The mechanism of hydrolysis of amino acyl RNA, *Biochemistry* 2, 1090–1092.
41. Sherlin, L. D., Bullock, T. L., Nissan, T. A., Perona, J. J., Lariviere, F. J., Uhlenbeck, O. C., and Scaringe, S. A. (2001) Chemical and enzymatic synthesis of tRNAs for high-throughput crystallization, *RNA* 7, 1671–1678.
42. Mulvey, R. S., and Fersht, A. R. (1977) Editing mechanisms in aminoacylation of tRNA: ATP consumption and the binding of aminoacyl-tRNA by elongation factor Tu, *Biochemistry* 16, 4731–4737.
43. Schowen, K. B., and Schowen, R. L. (1982) Solvent isotope effects of enzyme systems, *Methods Enzymol.* 87, 551–606.
44. Jencks, W. (1969) *Catalysis in Chemistry and Enzymology*, McGraw Hill Text.
45. Riesner, D., Pingoud, A., Boehme, D., Peters, F., and Maass, G. (1976) Distinct steps in the specific binding of tRNA to aminoacyl-tRNA synthetase. Temperature-jump studies on the serine-specific system from yeast and the tyrosine-specific system from *Escherichia coli*, *Eur. J. Biochem.* 68, 71–80.
46. Krauss, G., Riesner, D., and Maass, G. (1976) Mechanism of discrimination between cognate and non-cognate tRNAs by phenylalanyl-tRNA synthetase from yeast, *Eur. J. Biochem.* 68, 81–93.
47. Fersht, A. R. (1998) *Structure and Mechanism in Protein Science: A Guide to Enzyme Catalysis and Protein Folding*, 3rd ed., W. H. Freeman.
48. Anderson, B. M., Cordes, E. H., and Jencks, W. P. (1961) Reactivity and catalysis in reactions of the serine hydroxyl group and of O-acyl serines, *J. Biol. Chem.* 236, 455–463.
49. Schuber, F., and Pinck, M. (1974) On the chemical reactivity of aminacyl-tRNA ester bond. 3. Influence of ionic strength, spermidine and methanol on the rate of hydrolysis, *Biochimie* 56, 397–403.
50. Schuber, F., and Pinck, M. (1974) On the chemical reactivity of aminoacyl-tRNA ester bond. I. Influence of pH and nature of the acyl group on the rate of hydrolysis, *Biochimie* 56, 383–390.
51. Schuber, F., and Pinck, M. (1974) On the chemical reactivity of aminoacyl-tRNA ester bond. 2. Aminolysis by tris and diethanolamine, *Biochimie* 56, 391–395.